Proceedings of the Korean Nuclear Society Spring Meeting
Cheju, Korea, May 2001

Improved Negative Fixup with Cell Rebalance for Boltzmann-Fokker-Planck Transport Equation

Yoon Keun Choi and Nam Zin Cho

Korea Advanced Institute of Science and Technology
Department of Nuclear Engineering
373-1 Kusong-dong, Yusong-gu
Taejon, Korea 305-701

Abstract

The Boltzmann-Fokker-Planck (BFP) equation for highly anisotropic scattering problems such as charged particle transport combines the advantages of the Boltzmann transport equation and the Fokker-Planck equation. Because the BFP equation involves angular flux derivatives with respect to energy and direction, the standard neutron transport codes cannot be used directly to solve the BFP equation. The diamond difference scheme can be applied to the BFP equation with respect to energy and space. This scheme is accurate for finite mesh size, but it is subject to negative flux. If negative flux comes out of one mesh, then the solution can be completely wrong. So, the diamond difference scheme needs a negative flux fixup, and a conservative fixup scheme was used by Przybylski and Ligou. In this study, a negative flux fixup scheme with cell-rebalanced average flux is developed, improving the results of Przybylski and Ligou. Because the nonlinearity introduced by negative flux fixup has influence on solution, the nodal method (constant-constant) is also applied to the BFP equation with respect to energy and space. Since the nodal method is a more positive scheme than the diamond difference scheme, it can be an alternative for the BFP equation.

1. Introduction

The transport of neutrons or gamma rays in various media is governed by the Boltzmann equation. The scattering cross sections are expanded into Legendre polynomial series [1][2]. This assumes that scattering is almost isotropic. When scattering cross sections are highly anisotropic as for fast neutrons and for charged particles, Legendre expansion is unsuitable. To avoid such difficulties, Przybylski and Ligou[3] proposed the Boltzmann equation including Fokker-Planck terms (the BFP equation), which combines the advantages of the usual transport equations and the Fokker-Planck equation.

The BFP equation is suitable to describe behavior of highly anisotropic scattering problems. But, the BFP equation is different from the neutron transport equation and cannot be solved directly by standard neutron transport codes, because this equation involves angular flux derivatives with respect to energy and direction.

To find solution, the diamond difference scheme was applied to the BFP equation with respect to energy and space[3]. A review on the derivation and numerical methods for the BFP equation is provided in Ref. 4. The well-known diamond difference scheme is accurate to

second order, but the calculated fluxes can be negative. A procedure to avoid such behavior could be to reduce the mesh size, but it takes long time and it is difficult in practice to do that in an absolutely safe way. Even if negative flux comes out for only one mesh, then the solution can be completely wrong even in the case which the meshes are small enough. So, the diamond difference scheme needs the negative flux fixup. In this study, a new negative flux fixup scheme with cell-rebalanced average flux is developed.

The nonlinearity can have influence on solution such as oscillation, even though the negative flux fixup is performed. To avoid this fault, the nodal method (constant-constant)[5], which is known to be more positive, is also applied to the BFP equation with respect to energy and space. The nodal method can be an alternative for the BFP equation.

2. Derivation of Boltzmann-Fokker-Planck (BFP) Equation

2.1 Boltzmann-Fokker-Planck (BFP) Equation

The transport of neutron is governed by the linear Boltzmann equation. The scattering terms of the Boltzmann transport equation are expanded into Legendre polynomial series. This method assumes that the scattering cross sections are almost isotropic. But this approach is not good in the transport of particles such as proton, alpha particle and electron, because the scattering cross sections are so forward peaked that even Legendre expansions of high degree fail. To avoid such difficulties, one uses a linear Fokker-Planck equation. But the FP equation can't describe any large energy transfer. So one proposed new transport equation, called the Boltzmann-Fokker-Planck (BFP) equation, which combined the advantages of the Boltzmann equation and the Fokker-Planck equation.

The Boltzmann-Fokker-Planck (BFP) equation is derived from the usual neutron transport equation which is written as

$$\begin{aligned} &\left[\frac{1}{v}\frac{\partial}{\partial t} + \hat{\Omega}\cdot\nabla + \sigma(\vec{r},\hat{\Omega},E) \right]\psi(\vec{r},\hat{\Omega},E,t) \\ &= \int d\hat{\Omega}' \int_0^\infty dE' \sigma_s(\vec{r},E'\to E,\hat{\Omega}'\to\hat{\Omega})\psi(\vec{r},\hat{\Omega}',E',t) + Q. \end{aligned} \tag{1}$$

The scattering cross section can be split into two parts[6] as

$$\sigma = \sigma_s + \sigma_a = \sigma_{reg} + \sigma_{sing} + \sigma_a, \tag{2}$$

where

v	:	neutron velocity,
σ	:	total cross section,
σ_s	:	scattering cross section,
σ_{reg}	:	smooth component of scattering cross section,
σ_{sing}	:	singular component of scattering cross section,
σ_a	:	absorption cross section,
Q	:	external source.

The "regular cross section"(reg) in Eq. (2) is a smooth function of the scattering angle cosine, which generates a small number of Legendre functions. The "singular cross section"(sing) in

Eq. (2) takes very large values for $\mu_0 = \hat{\Omega} \cdot \hat{\Omega}' \simeq 1$. The BFP Equation in slab geometry can be written[3] as

$$\begin{aligned} \frac{1}{v}\frac{\partial \psi}{\partial t} &+ \mu \frac{\partial \psi}{\partial x} + (\sigma_{reg} + \sigma_a)\psi \\ &= \sum_{l=0}^{\infty} \frac{2l+1}{2} P_l(\mu) \int_0^{\infty} \sigma_{reg,l}(E' \to E)\phi_l(E')dE' \\ &+ \frac{\partial}{\partial E} S\psi + T\frac{\partial}{\partial \mu}(1-\mu^2)\frac{\partial \psi}{\partial \mu} + Q. \end{aligned} \tag{3}$$

The coefficients S, which is called restricted momentum transfer, and T, which is called stopping power, of the BFP equation can be written as

$$\begin{aligned} T(E) &= \frac{1}{4}\int_0^{\infty} dE' \int_{-1}^{1} d\mu_0 (1-\mu_0)\sigma_{sing}(\vec{r}, E \to E', \mu_0), \\ S(E) &= \frac{1}{2}\int_0^{\infty} (E-E')dE' \int_{-1}^{1} d\mu_0 \sigma_{sing}(\vec{r}, E \to E', \mu_0). \end{aligned} \tag{4}$$

2.2 Angle Discretization

The discrete ordinates method is applied to the μ variable and for each direction μ_k a weighting factor w_k is given[1][2]. Then the parabolic term in Eq. (3) becomes

$$T(A_k\psi_{k-1}^n - B_k\psi_k^n + C_k\psi_{k+1}^n) \quad \text{for } k = 1, 2, \ldots, K, \tag{5}$$

with

$$\begin{aligned} A_k &= \frac{1-\mu_{k-1/2}^2}{w_k(\mu_k - \mu_{k-1})}, \\ B_k &= A_k + C_k, \\ C_k &= \frac{w_{k+1}}{w_k} A_{k+1}, \\ w_k &= \mu_{k+1/2} - \mu_{k-1/2}, \\ \mu_{1/2} &= -1 \quad , \quad \mu_{K+1/2} = 1. \end{aligned} \tag{6}$$

Eq. (3) can be written as

$$\begin{aligned} \mu_k \frac{\partial}{\partial x}\psi_k &- \frac{\partial}{\partial E} S\psi_k = -(\sigma_{reg} + \sigma_a + TB_k)\psi_k \\ &+ T\ (A_k\psi_{k-1} + C_k\psi_{k+1}) + q_k + Q_k, \end{aligned} \tag{7}$$

where

$$\begin{aligned} q_k &= \sum_{l=0}^{\infty} \frac{2l+1}{2} P_l(\mu) \int_0^{\infty} \sigma_{reg,l}(E' \to E)\phi_l(E')dE', \\ \phi_l &= \sum_{k=0}^{K} w_k P_l(\mu_k)\psi_k. \end{aligned} \tag{8}$$

2.3 FP Coefficients

The usual cross section must be corrected since it does not deal with the singular part of differential scattering cross section, and the procedure to calculate the FP coefficients has to be defined[6]. In most libraries, neutron transfers only from one group to next are assumed to be possible for heavy nuclides. So, Caro and Ligou restrict cross sections due to this assumption, even though it is possible to determine others. Due to the above assumption, only two matrix elements have to be determined in each group: $\sigma_{s,l}(g \to g)$ and $\sigma_{s,l}(g \to g+1)$.

$\sigma_{s,l}(g \to g')$ is obtained from BUGLE-96 Library[7]. But $\sigma_{s,l}(g \to g)$ and $\sigma_{s,l}(g \to g+1)$ are available and the Legendre moments of the scattering cross section for group g are written as

$$\sigma_{s,l}(g) = \sigma_{s,l}(g \to g) + \sigma_{s,l}(g \to g+1). \tag{9}$$

If l is large enough, they set

$$\sigma_{s,l}(g) = \sigma^{''}_{s,l}(g) \quad , \; l \geq 5. \tag{10}$$

We can set $\sigma_{s,l}(g) = \sigma^{''}_{s,l}(g)$ for $l = L$ and $l = L-1$; then we obtain

$$\frac{\sigma_{s,L-1}}{\sigma_{s,L}} = \frac{\sigma^{''}_{s,L-1}}{\sigma^{''}_{s,L}} = \frac{h_{L-1}(\tau^{''})}{h_L(\tau^{''})}, \tag{11}$$

where the first ratio is known, and

$$\begin{aligned} h_0(\tau) &= 1 - exp(-2\tau), \\ h_1(\tau) &= 1 - \frac{1}{\tau} + \left(1 + \frac{1}{\tau}\right) exp(-2\tau), \\ h_l(\tau) &= h_{l-2}(\tau) - \frac{2l-1}{\tau} h_{l-1}(\tau). \end{aligned} \tag{12}$$

We can find $\tau^{''}$ by trial and error. Eq. (11) provides all $\tau^{''}(g)$, and we obtain coefficients $\sigma^{''}_{s,l}$:

$$\sigma^{''}_{s,l}(g) = \frac{\sigma^{''}_{s,L}(g) h_l(\tau^{''}_g)}{h_L(\tau^{''}_g)}. \tag{13}$$

and $\sigma''_{s,l}$ will be different from $\sigma_{s,l}$ except for L. Finally, the singular cross section can be determined as follows:

$$\sigma''_{s,l}(g \to g+1) = \frac{2}{Aln(\frac{E_{g-1}}{E_g})} \sigma''_{s,l}(g) \frac{g_l(\tau''_g)}{h_L(\tau''_g)}, \tag{14}$$

where

$$g_l(\tau) = (1 - \frac{1}{\tau}) h_l(\tau) - h_{l+1}(\tau), \tag{15}$$

and

$$\sigma''_{s,l}(g \to g) = \sigma''_{s,l}(g) - \sigma''_{s,l}(g \to g+1). \tag{16}$$

The regular cross sections are given by

$$\begin{aligned} \sigma'_{s,l}(g \to g) &= \sigma_{s,l}(g \to g) - \sigma''_{s,l}(g \to g), \\ \sigma'_{s,l}(g \to g+1) &= \sigma_{s,l}(g \to g+1) - \sigma''_{s,l}(g \to g+1), \quad l < L. \end{aligned} \tag{17}$$

The restricted moment transfer($T(E_g)$) and stopping power($S(E_g)$) are then given by

$$\begin{aligned} T(E_g) &= \frac{1}{2}(\sigma''_{s,0}(g) - \sigma''_{s,1}(g)), \\ S(E_g) &= \frac{4E_g}{A} T(E_g). \end{aligned} \tag{18}$$

3. New Negative Fixup Scheme with Cell Rebalance in Diamond Difference Method

3.1 Derivation of Diamond Difference Scheme

The diamond approximation is accurate to second order and this scheme can be applied to the BFP equation for space-energy mesh [3][4]. But the calculated fluxes can be negative. To protect this phenomena, this scheme needs the negative flux fixup.

Let's consider a mesh in the (x, E) space (Fig. 1.)

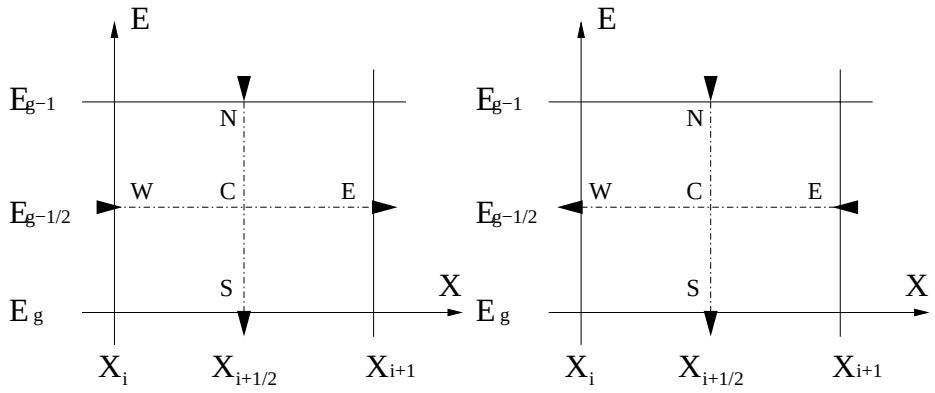

(a) $\mu_k > 0$ (b) $\mu_k < 0$

Fig. 1. Definition of two-dimensional meshes for the diamond difference scheme.

$$\begin{aligned} \psi_{C,k} &= \psi(x_{i+1/2}, E_{g-1/2}, \mu_k), \\ \psi_{N,k} &= \psi(x_{i+1/2}, E_{g-1}, \mu_k) \ , \ \psi_{S,k} = \psi(x_{i+1/2}, E_g, \mu_k), \\ \psi_{W,k} &= \psi(x_i, E_{g-1/2}, \mu_k) \ , \ \psi_{E,k} = \psi(x_{i+1}, E_{g-1/2}, \mu_k), \end{aligned} \tag{19}$$

$$\begin{aligned} \text{space} &: \ i = 1, 2, \ldots, I, \\ \text{energy} &: \ g = 1, 2, \ldots, G, \\ \text{angle} &: \ k = 1, 2, \ldots, K. \end{aligned}$$

After integration over (x, E) mesh, and dividing by $\triangle x = x_{i+1} - x_i$ and $\triangle E = E_{g-1} - E_g$, Eq. (7) can be written as

$$\mu_k \frac{\psi_{E,k} - \psi_{W,k}}{\triangle x} - \frac{S_N \psi_{N,k} - S_S \psi_{S,k}}{\triangle E} = F_{C,k}, \tag{20}$$

where

$$\begin{aligned} F_{C,k} &= -(\sigma_{reg} + \sigma_a + TB_k)_C \psi_{C,k} + T_C(A_k \psi_{C,k-1} + C_k \psi_{C,k+1}) \\ &\quad + q_{C,k} + Q_{C,k}, \\ q_{C,k} &= \sum_{l=0}^{L} \frac{2l+1}{2} P_l(\mu_k) \sum_{h=1}^{G} \sigma_{reg,h\to g,l} \phi_{h,l}, \\ \phi_{g,l} &= \sum_{k=1}^{K} w_k P_l(\mu_k) \psi_{g,k}. \end{aligned} \tag{21}$$

The usual diamond difference scheme is introduced:

$$2\psi_{C,k} = \psi_{W,k} + \psi_{E,k} = \psi_{N,k} + \psi_{S,k} \tag{22}$$

By inserting Eq. (22) into Eq. (20), $\psi_{S,k}$ and $\psi_{E,k}$ or $\psi_{W,k}$ are eliminated. Eq. (20) can be written as

$$\begin{aligned} -T_C A_k \psi_{C,k-1} + \left[2\frac{|\mu_k|}{\triangle x} + 2\frac{S_S}{\triangle E} + \left(\sigma_{reg} + \sigma_a + TB_k \right)_C \right] \psi_{C,k} - T_C C_k \psi_{C,k+1} \\ = 2\frac{|\mu_k|}{\triangle x} \psi_{W,k} + \frac{S_N + S_S}{\triangle E} \psi_{N,k} + q_{C,k} + Q_{C,k} \quad \text{for} \quad \mu_k > 0. \end{aligned} \tag{23}$$

The calculations are started from the highest energy and from the left or right boundaries of the system according to the sign of μ_k. Eq. (23) provides all angular fluxes in a given mesh ($\psi_{C,k}$). Then the edge values $\psi_{S,k}$ and $\psi_{E,k}$ (or $\psi_{W,k}$) are computed through Eq. (22). Even though Eq. (23) gives positive fluxes, $\psi_{C,k}$, $\psi_{S,k}$ or ($\psi_{E,k}$ or $\psi_{W,k}$) in Eq. (22) can be negative. A way to avoid such behavior is to reduce the mesh sizes, but it is difficult in practice to do that in an absolutely safe way. Even if only one mesh provides a negative edge flux, the solution can be quite wrong. So the diamond difference scheme needs negative flux fixup, and a conservative fixup was proposed by Przybylski and Ligou. In this study a new fixup scheme with cell-rebalanced average flux is developed.

3.2 Conservative Fixup by Przybylski and Ligou

When Eq. (22) provides negative flux, it is not good to assign a zero value to the negative fluxes because the particle and energy balances would not be preserved. So Przybylski and Ligou developed "conservative fixup"[3]. The balance equation is

$$\mu_k \frac{\psi_{E,k} - \psi_{W,k}}{\Delta x} - \frac{S_N \psi_{N,k} - S_S \psi_{S,k}}{\Delta E} = F_{C,k}, \quad \text{for} \quad \mu_k > 0, \tag{24}$$

where

$$\begin{aligned} F_{C,k} &= -\sigma^*_{C,k} \psi_{C,k} + R_{C,k}, \\ R_{C,k} &= T_C(A_k \psi_{C,k-1} + C_k \psi_{C,k+1}) + q_{C,k} + Q_{C,k}, \\ \sigma^*_{C,k} &= \sigma_{reg} + \sigma_a + TB_k. \end{aligned} \tag{25}$$

If we set the correction of negative flux as,

$$\psi_{S,k} = \tilde{\psi}_{S,k} + \epsilon_{S,k} \text{ and } \psi_{E,k} = \tilde{\psi}_{E,k} + \epsilon_{E,k}, \tag{26}$$

we can rewrite balance equation as

$$\mu_k \frac{\tilde{\psi}_{E,k} - \psi_{W,k}}{\Delta x} - \frac{S_N \psi_{N,k} - S_S \tilde{\psi}_{S,k}}{\Delta E} + \frac{\epsilon_{S,k} S_S}{\Delta E} + \mu_k \frac{\epsilon_{E,k}}{\Delta x} = F_{C,k}. \tag{27}$$

To preserve balance, we obtain

$$\frac{\epsilon_{S,k} S_S}{\Delta E} + \mu_k \frac{\epsilon_{E,k}}{\Delta x} = 0, \tag{28}$$

where $\epsilon_{E,k}$ is replaced by $\epsilon_{W,k}$ if $\mu_k < 0$. When a negative value $\psi_{E,k}$ comes out, we set $\tilde{\psi}_{E,k} = 0$ ($\epsilon_{E,k} = \psi_{E,k}$). We must also correct $\psi_{S,k}$ due to Eq. (28) as

$$\tilde{\psi}_{S,k} = \psi_{S,k} - \epsilon_{S,k} = \psi_{S,k} + |\mu_k| \frac{\Delta E \epsilon_{E,k}}{\Delta x S_S} = \psi_{S,k} + |\mu_k| \frac{\Delta E \psi_{E,k}}{\Delta x S_S}. \tag{29}$$

When a negative value $\psi_{S,k}$ comes out, we set $\tilde{\psi}_{S,k} = 0$ ($\epsilon_{S,k} = \psi_{S,k}$) in the same way. We must also correct $\psi_{E,k}$ as

$$\tilde{\psi}_{E,k} = \psi_{E,k} - \epsilon_{E,k} = \psi_{E,k} + S_S \frac{\Delta x \epsilon_{S,k}}{\Delta E |\mu_k|} = \psi_{E,k} + S_S \frac{\Delta x \psi_{S,k}}{\Delta E |\mu_k|}. \tag{30}$$

3.3 New Fixup Scheme with Cell-Rebalanced Average Flux

The conservative fixup does not consider average flux $\psi_{C,k}$, when the edge fluxes are corrected. If the edge fluxes $\psi_{S,k}$ or $\psi_{E,k}(\psi_{W,k})$ are corrected, the average flux $\psi_{C,k}$ should also be corrected. The balance equation is

$$\mu_k \frac{\psi_{E,k} - \psi_{W,k}}{\Delta x} - \frac{S_N \psi_{N,k} - S_S \psi_{S,k}}{\Delta E} + \sigma^*_{C,k} \psi_{C,k} = R_{C,k}. \tag{31}$$

If the correction of negative flux and average flux are set as ($\mu_k > 0$),

$$\begin{aligned} \text{Negative Flux} &: \psi_{S,k} = \tilde{\psi}_{S,k} + \epsilon_{S,k}, \quad \text{and} \quad \psi_{E,k} = \tilde{\psi}_{E,k} + \epsilon_{E,k}, \\ \text{Average Flux} &: \psi_{C,k} = \tilde{\psi}_{C,k} + \epsilon_{C,k}, \end{aligned} \tag{32}$$

the balance equation can be rewritten as

$$\begin{aligned} &\mu_k \frac{\tilde{\psi}_{E,k} - \psi_{W,k}}{\Delta x} - \frac{S_N \psi_{N,k} - S_S \tilde{\psi}_{S,k}}{\Delta E} + \sigma^*_{C,k} \tilde{\psi}_{C,k} \\ &+ \frac{\mu_k \epsilon_{E,k}}{\Delta x} + \frac{S_S \epsilon_{S,k}}{\Delta E} + \sigma^*_{C,k} \epsilon_{C,k} = R_{C,k}. \end{aligned} \tag{33}$$

To preserve balance, the following relation is obtained as

$$\frac{\mu_k \epsilon_{E,k}}{\Delta x} + \frac{S_S \epsilon_{S,k}}{\Delta E} + \sigma^*_{C,k} \epsilon_{C,k} = 0. \tag{34}$$

When a negative value of $\psi_{E,k}$ comes out, one set $\tilde{\psi}_{E,k} = 0$ ($\epsilon_{E,k} = \psi_{E,k}$). One must correct $\psi_{S,k}$, and $\psi_{C,k}$ due to Eq. (34) for $\mu_k > 0$. The average flux in the diamond difference scheme is

$$\psi_{C,k} = \frac{\psi_{S,k} + \psi_{N,k}}{2}. \tag{35}$$

If a negative flux ($\psi_{E,k}$) is corrected, Eq. (35) is written as

$$\tilde{\psi}_{C,k} + \epsilon_{C,k} = \frac{\tilde{\psi}_{S,k} + \psi_{N,k}}{2} + \frac{\epsilon_{S,k}}{2}. \tag{36}$$

We also set the balance for corrected fluxes such as

$$\tilde{\psi}_{C,k} = \frac{\tilde{\psi}_{S,k} + \psi_{N,k}}{2}. \tag{37}$$

From Eqs. (36) and (37), we get

$$2\epsilon_C = \epsilon_S. \tag{38}$$

By inserting Eq. (38) into Eq. (34), $\epsilon_{C,k}$ is eliminated and $\epsilon_{S,k}$ is written as

$$\epsilon_{S,k} = -\frac{|\mu_k|/\triangle x}{S_S/\triangle E + \sigma^*_{C,k}/2}\epsilon_{E,k}. \tag{39}$$

The corrected fluxes are

$$\begin{aligned} \tilde{\psi}_{S,k} &= \psi_{S,k} - \epsilon_{S,k} = \psi_{S,k} + \frac{|\mu_k|/\triangle x}{S_S/\triangle E + \sigma^*_{C,k}/2}\psi_{E,k}, \\ \tilde{\psi}_{C,k} &= \psi_{C,k} - \epsilon_{C,k} = \psi_{C,k} + \frac{1}{2}\frac{|\mu_k|/\triangle x}{S_S/\triangle E + \sigma^*_{C,k}/2}\psi_{E,k}. \end{aligned} \tag{40}$$

When a negative value of $\psi_{S,k}$ comes out, one set $\tilde{\psi}_{S,k} = 0$ ($\epsilon_{S,k} = \psi_{S,k}$) in the same way. Now one must correct $\psi_{E,k}$, and $\psi_{C,k}$. The average flux is expressed as

$$\psi_{C,k} = \frac{\psi_{E,k} + \psi_{W,k}}{2}. \tag{41}$$

If a negative flux ($\psi_{S,k}$) is corrected, Eq. (41) is written as

$$\tilde{\psi}_{C,k} + \epsilon_{C,k} = \frac{\tilde{\psi}_{E,k} + \psi_{W,k}}{2} + \frac{\epsilon_{E,k}}{2}. \tag{42}$$

To preserve balance, we get

$$2\epsilon_{C,k} = \epsilon_{E,k}. \tag{43}$$

By inserting Eq. (43) into Eq. (34), $\epsilon_{C,k}$ is eliminated, and $\epsilon_{E,k}$ is written as

$$\epsilon_{E,k} = \frac{S_S/\Delta E}{|\mu_k|/\Delta x + \sigma^*_{C,k}/2}\epsilon_{S,k}. \tag{44}$$

The corrected fluxes are

$$\begin{aligned}\tilde{\psi}_{E,k} &= \psi_{E,k} - \epsilon_{E,k} = \psi_{E,k} + \frac{S_S/\Delta E}{|\mu_k|/\Delta x + \sigma^*_{C,k}/2}\psi_{S,k},\\ \tilde{\psi}_{C,k} &= \psi_{C,k} - \epsilon_{C,k} = \psi_{C,k} + \frac{1}{2}\frac{S_S/\Delta E}{|\mu_k|/\Delta x + \sigma^*_{C,k}/2}\psi_{S,k}.\end{aligned} \tag{45}$$

If negative flux of $\psi_{E,k} < 0$ and $\psi_{S,k} < 0$ comes out, one set $\tilde{\psi}_{E,k} = 0$ $\tilde{\psi}_{S,k} = 0$. And the average flux is

$$\tilde{\psi}_{C,k} = \frac{R_{C,k} + |\mu_k|\frac{\psi_{W,k}}{\Delta x} + \frac{S_N\psi_{N,k}}{\Delta E}}{\sigma^*_{C,k}}, \tag{46}$$

due to the balance Eq. (33).

4. Nodal Method (Constant-Constant)

The diamond difference scheme has a weak point to produce negative flux for coarse mesh size. But there is relatively low possibility to produce negative flux in the nodal method (constant-constant) for coarse mesh size[4][5]. The term "constant-constant" means that the angular flux shape is assumed to be constant in cell and on edge. The BFP balance equation for (x, E) geometry is given by

$$\mu_k\frac{\partial}{\partial x}\psi_k - \frac{\partial}{\partial E}S\psi_k + \sigma^*_t\psi_k = T\left(A_k\psi_{k-1} + C_k\psi_{k+1}\right) + q_k, \tag{47}$$

where

$$\sigma^*_t = \sigma_{reg} + \sigma_a + TB_k. \tag{48}$$

$T\left(A_k\psi_{k-1} + C_k\psi_{k+1}\right) + q_k$ is assumed to be constant. If $\mu_k > 0$, then the angular fluxes on the left and top edges are known. Next, Eq. (47) is integrated from E_g to E_{g-1}:

$$\mu_k\frac{\partial}{\partial x}\bar{\psi}_k(x) + \sigma^*_t\bar{\psi}_k(x) = S_C\frac{\psi_{S,k} - \psi_{N,k}}{\triangle E} + T\left(A_k\psi_{k-1} + C_k\psi_{k+1}\right) + q_k. \tag{49}$$

where

$$\bar{\psi}_k(x) = \frac{1}{\Delta E}\int_{E_g}^{E_{g-1}}\psi_k(x, E)dE. \tag{50}$$

Integrating Eq. (49) for x-direction in the space mesh gives the outgoing angular flux on the right edge:

$$\begin{aligned}\psi_{E,k} =& e^{-\epsilon^x}\psi_{W,k} + \frac{1}{\sigma^*_t}(1 - e^{-\epsilon^x})\\ &\times\left(\frac{S_C}{\Delta E}(\psi_{S,k} - \psi_{N,k}) + T\left(A_k\psi_{k-1} + C_k\psi_{k+1}\right) + q_k\right),\end{aligned} \tag{51}$$

where

$$\epsilon^x = \frac{\sigma^*_t\Delta x}{|\mu_k|}. \tag{52}$$

For simplicity, Eq. (51) and its counterpart for E-direction are rewritten as:

$$\begin{aligned}\psi_{E,k} &= e^{-\epsilon^x}\psi_{W,k} + b^{'x}(T\,(A_k\psi_{k-1} + C_k\psi_{k+1}) + q_k)) \\ &\quad + a^{'x}(\psi_{S,k} - \psi_{N,k}), \\ \psi_{S,k} &= e^{-\epsilon^g}\psi_{N,k} + b^{'g}(T\,(A_k\psi_{k-1} + C_k\psi_{k+1}) + q_k) \\ &\quad + a^{'g}(\psi_{E,k} - \psi_{W,k}),\end{aligned} \tag{53}$$

where

$$\begin{aligned}a^{'x} &= \frac{1}{\epsilon^g}(1 - e^{-\epsilon^x}) \quad , \quad b^{'x} = \frac{1}{\sigma_t^*}(1 - e^{-\epsilon^x}), \\ a^{'g} &= \frac{1}{\epsilon^x}(1 - e^{-\epsilon^g}) \quad , \quad b^{'g} = \frac{1}{\sigma_t^*}(1 - e^{-\epsilon^g}), \\ \epsilon^g &= \frac{\sigma_t^*\Delta E}{S_C}.\end{aligned} \tag{54}$$

Eq. (53) is solved for the outgoing angular fluxes (i.e., $\psi_{E,k}, \quad \psi_{S,k}$) that are represented in terms of the incoming angular fluxes and sources. The equations are given by

$$\begin{aligned}\psi_{E,k} &= a^x\psi_{W,k} + b^x\psi_{N,k} + c^xQ_k, \\ \psi_{S,k} &= a^g\psi_{N,k} + b^g\psi_{W,k} + c^gQ_k.\end{aligned} \tag{55}$$

where

$$\begin{aligned}a^x &= \frac{e^{-\epsilon^x} - a^{'x}a^{'g}}{1 - a^{'x}a^{'g}} \ , \ b^x = \frac{(1 - e^{-\epsilon^g})a^{'x}}{1 - a^{'x}a^{'g}} \ , \ c^x = \frac{b^{'x} - a^{'x}b^{'g}}{1 - a^{'x}a^{'g}}, \\ a^g &= \frac{e^{-\epsilon^g} - a^{'g}a^{'x}}{1 - a^{'g}a^{'x}} \ , \ b^g = \frac{(1 - e^{-\epsilon^x})a^{'g}}{1 - a^{'g}a^{'x}} \ , \ c^g = \frac{b^{'g} - a^{'g}b^{'x}}{1 - a^{'g}a^{'x}}.\end{aligned} \tag{56}$$

5. Numerical Test and Results

5.1 Test Problem 1 (U^{238} Slab)

The configuration is given in Fig. 2, which is a homogeneous shielding problem. P_5 scattering is available and S_{16} Gauss-Legendre quadratures are used. The density of U^{238} is $10^{24}\#/cm^3$ and convergence criterion is 10^{-8}. Reference calculation is performed by the diamond difference scheme with a fine mesh size of fine $0.01cm$. We test two kinds of fixup methods (Ligou's fixup and new fixup methods). The nodal method(C-C) is also applied, which gives almost positive solutions.

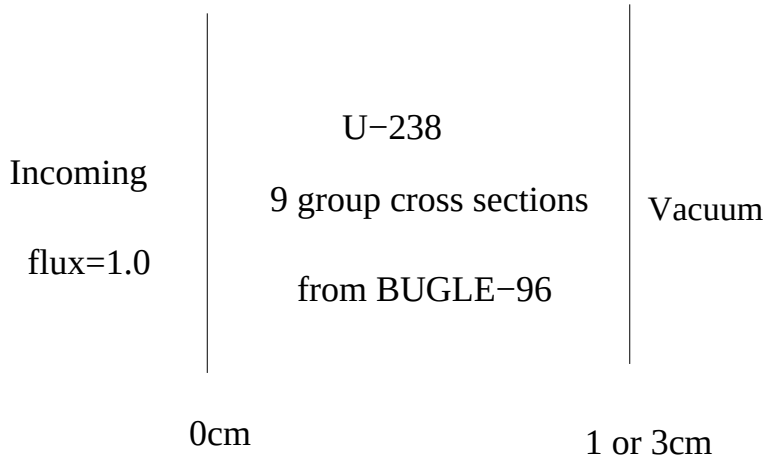

Fig. 2. Configuration of test problem 1.

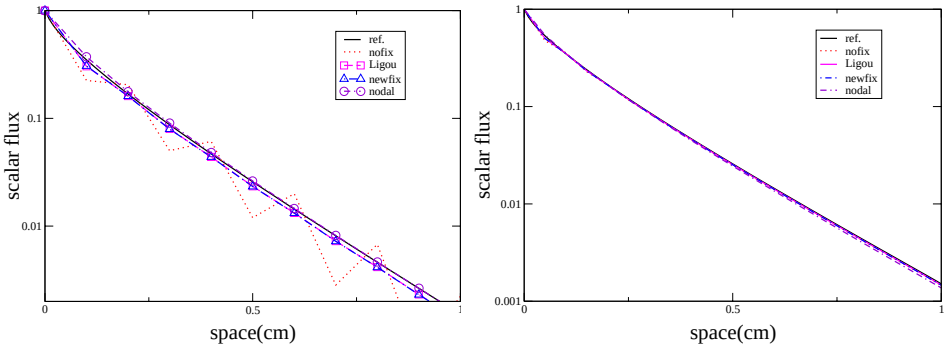

(a) group 1, mesh size= 0.1 (b) group 1, mesh size= 0.05

Fig. 3. Distribution of scalar flux for interval $0 < x < 1$.

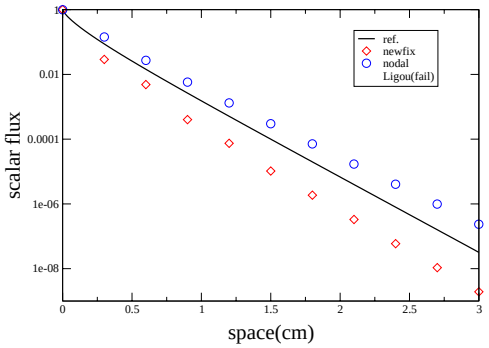

Fig. 4. Distribution of scalar flux for interval $0 < x < 3$.
(group 1, mesh size= 0.3)

The diamond difference scheme shows oscillation for coarse mesh size (Fig. 3). So, this scheme needs negative flux fixup for coarse mesh size. New fixup method as well as Ligou's fixup method works successfully for the mesh size of 0.05 and $0.1cm$. Ligou's fixup method does not converge for the mesh size of $0.3cm$, but new fixup method converges well (Fig. 4). This results show that new fixup is more improved than Ligou's fixup for coarse mesh size problem. In test problem1, Ligou's method converges until mesh size of $0.25cm$ but new method converges until mesh size of $0.36cm$.

The nodal method works successfully for various mesh sizes (0.05, $0.1cm$) and converges for mesh size($0.3cm$).

5.2 Test Problem 2 (U^{238} and Zr^{91} Slab)

The second test is a heterogeneous slab geometry problem, as shown in Fig. 5. P_5 scattering is available and S_{16} Gauss-Legendre quadratures are used. The density of U^{238} and Zr^{91} are both $10^{24}\#/cm^3$ and error criterion is 10^{-8}. The diamond difference scheme (Ligou's fixup and new fixup methods) and the nodal method are applied. The results of fine mesh calculations are obtained when the mesh size is $0.04cm$.

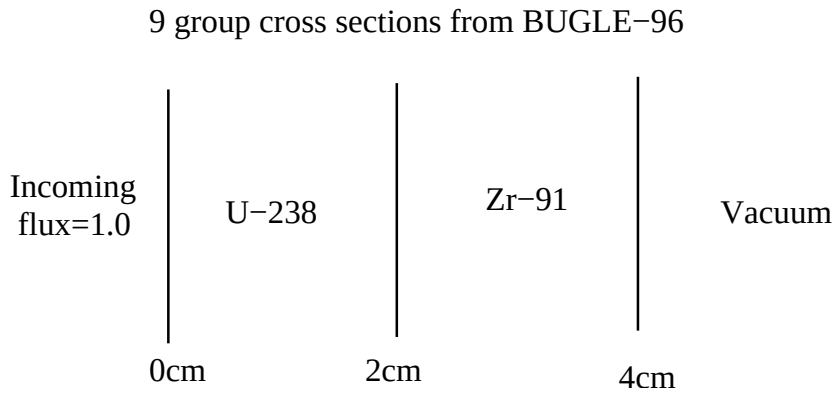

Fig. 5. Configuration of test problem 2.

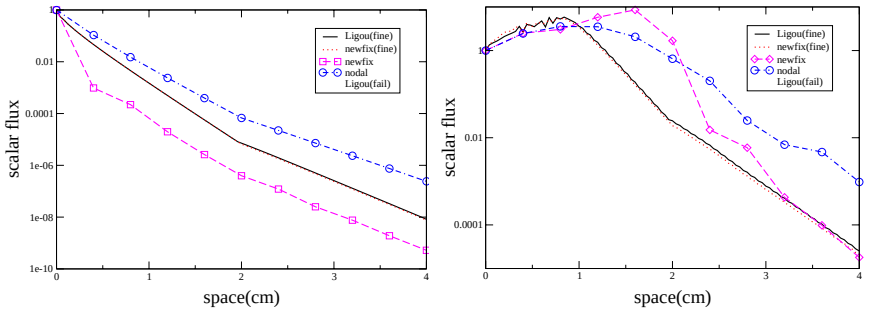

(a) group 1, mesh size= 0.4 (b) group 9, mesh size= 0.4

Fig. 6. Distribution of scalar flux for interval $0 < x < 4$.

In test problem2, Ligou's method converges until mesh size of $0.25cm$ but new method converges until mesh size of $0.4cm$. The nodal method converges successfully too.

6. Conclusions

The BFP equation is suitable to describe the behavior of highly anisotropic scattering problems such as the transport of fast neutrons and charged particles. The BFP equation is different from the Boltzmann neutron transport equation and cannot be solved by the standard neutron transport codes, because this equation involves angular flux derivatives with respect to energy and direction.

The well-known diamond difference scheme having second order accuracy is applied to the BFP equation with respect to energy and space, but unfortunately the calculated flux is not always positive. To avoid this behavior, mesh size has to be reduced, but there still exists possibility of getting negative flux. Because even only one negative flux can make the solution wrong, the diamond difference scheme needs negative flux fixup. In this study, a new negative fixup method with cell-rebalanced average flux was developed. This new fixup is an improved method, that is more accurate than the Ligou's approach for coarse mesh size.

Though the negative flux fixup is performed, the nonlinearity may have influence on the solution such as oscillation. So, the nodal method was also applied to the BFP equation. It is known that the nodal method produces nearly positive solutions. When the nodal method was applied to the BFP equation, the solutions were positive even in coarse mesh size. So, the nodal method can be an alternative for the BFP equation.

Acknowledgement

This work was supported in part by the Ministry of Science and Technology of Korea through the National Research Laboratory (NRL) Program.

References

[1] E. E. Lewis and W. F. Miller, Jr., *Computational Methods of Neutron Transport*, John Wiley & Sons, 1984.

[2] K. M. Case and P. F. Zweifel, *Linear Transport Theory*, Addison-Wesley Publishing Company, Inc., 1967.

[3] K. Przybylski and J. Ligou, "Numerical Analysis of the Boltzmann Equation Including Fokker-Planck Terms", *Nucl. Sci. Eng.*, **81**, 92-109, 1982.

[4] Nam Zin Cho and Ser Gi Hong, *Neutron Transport Theory-Computational Algorithms and Applications*, Chungmoongak, 2000 (in Korean).

[5] W. F. Walters and R. D. O'Dell, "Nodal Methods for Discrete-Ordinates Transport Problems in (x, y) Geometry", *Proc. Int. Topl. Mtg. Advances in Mathematical Methods for the Solution of Engineering Problems*, Munich, FRG, April 27-29, 1981, Vol. I, p. 115, American Nuclear Society, 1981.

[6] M. Caro and J. Ligou, "Treatment of Scattering Anisotropy of Neutrons Through the Boltzmann-Fokker-Planck Equation", *Nucl. Sci. Eng.*, **83**, 242, 1983.

[7] J. E. White, et. al., "Production and Testing of the Revised VITAMIN-B6 Fine-Group and the BUGLE-96 Broad-Group Neutron/Photon Cross-Section Libraries Derived from ENDF/BVI.3 Nuclear Data", ORNL-6795, R1, NUREG/CR-6214, Revision 1 (January 1995)(Draft)

[8] P. A. Haldy and J. Ligou, "A Moment Method for Calculating the Transport of Energetic Charged Particles in Hot Plasmas", *Nuclear Fusion*, **176**, 1125, 1977.

[9] P. A. Haldy and J. Ligou, "A Multigroup Formalism to Solve the Fokker-Planck Equation Characterizing Charged Particle Transport", *Nucl. Sci. Eng.*, **74**, 178-184, 1980.

[10] T. M. Tran and J. Ligou, "An Accurate Numerical Method to Solve the Linear Fokker-Planck Equation Characterizing Charged Particle Transport in Spherical Plasmas", *Nucl. Sci. Eng.*, **79**, 269-277, 1981.

[11] J. E. Morel, "Fokker-Planck Calculation Using Standard Discrete Ordinates Transport Code", *Nucl. Sci. Eng.*, **79**, 340, 1981.